

# A Highly Selective Electrochemical DNA-Based Sensor That Employs Steric Hindrance Effects to Detect Proteins Directly in Whole Blood

Sahar Sadat Mahshid,<sup>†</sup> Sébastien Camiré,<sup>†</sup> Francesco Ricci,<sup>‡</sup> and Alexis Vallée-Bélisle<sup>\*,†</sup>

<sup>†</sup>Laboratory of Biosensors & Nanomachines, Département de Chimie, Université de Montréal, Montréal, Québec H3T 1J4, Canada

<sup>‡</sup>Dipartimento di Scienze e Tecnologie Chimiche, University of Rome Tor Vergata, Rome 00133, Italy

**S** Supporting Information

**ABSTRACT:** Here we describe a highly selective DNA-based electrochemical sensor that utilizes steric hindrance effects to signal the presence of large macromolecules in a single-step procedure. We first show that a large macromolecule, such as a protein, when bound to a signaling DNA strand generates steric hindrance effects, which limits the ability of this DNA to hybridize to a surface-attached complementary strand. We demonstrate that the efficiency of hybridization of this signaling DNA is inversely correlated with the size of the molecule attached to it, following a semilogarithmic relationship. Using this steric hindrance hybridization assay in an electrochemical format (eSHHA), we demonstrate the multiplexed, quantitative, one-step detection of various macromolecules in the low nanomolar range, in <10 min directly in whole blood. We discuss the potential applications of this novel signaling mechanism in the field of point-of-care diagnostic sensors.

Current methods for the quantitative detection of protein markers, such as antibodies, still mostly rely on enzyme-linked immunosorbent assays (ELISAs),<sup>1</sup> Western blots,<sup>2</sup> and polarization assays,<sup>3</sup> which are multistep, wash- and reagent-intensive processes that necessitate specialized technicians and require several hours before completion. The development of rapid, low cost, point-of-care (POC) approaches for the quantitative detection of multiple proteins or biomarkers would drastically impact global health by allowing more frequent testing and by improving the penetration of molecular diagnostics into the developing world.<sup>4</sup> Current POC approaches, such as immunochemical dipsticks, display important advantages in terms of ease-of-use and affordability. Unfortunately, these remain hardly multiplexable for numerous targets, and their results remain mostly qualitative.<sup>4a,b,5</sup>

Over the past decade, many single-step homogeneous assays, have been explored to achieve multiplexed quantitative POC protein detection.<sup>6</sup> Those methods generally include protein-based<sup>7</sup> and DNA-based<sup>8</sup> assays (see reviews in refs 6 and 9). Among these single-step methods, DNA-based electrochemical sensors hold great promise.<sup>10</sup> These sensors are typically rapid, reagentless, multiplexable, and versatile, allowing detection of nucleic acids, proteins, and small analytes.<sup>8c</sup> However, these sensors still display significant nonspecific signal drift when immersed directly in whole blood, restricting their transition as POC diagnostic sensors.<sup>11</sup>

In response, we introduce here a novel versatile, highly selective, signal transduction mechanism that exploits steric hindrance effects at the nanoscale. Steric effects arise when atoms are brought close together. This creates an associated cost in energy due to overlapping electron clouds, which may affect the conformation and reactivity of molecules.<sup>12</sup> Here we propose to take advantage of such steric effects to alter the reactivity (hybridization efficiency) between two DNA strands. More specifically, we hypothesize that when a large macromolecule (e.g., >5 nm versus the relatively small ~2.4 nm diameter of DNA double helix) binds to a DNA strand, this should, in principle, reduce the number of DNA strands that can hybridize to their complementary strand attached to a surface at high density. We set out to demonstrate this steric hindrance mechanism using electrochemistry by employing a redox-labeled signaling DNA strand and a gold electrode that contains the complementary “capturing” DNA sequence at high surface density (Figure 1). Upon binding to the capturing strands, the redox-labeled

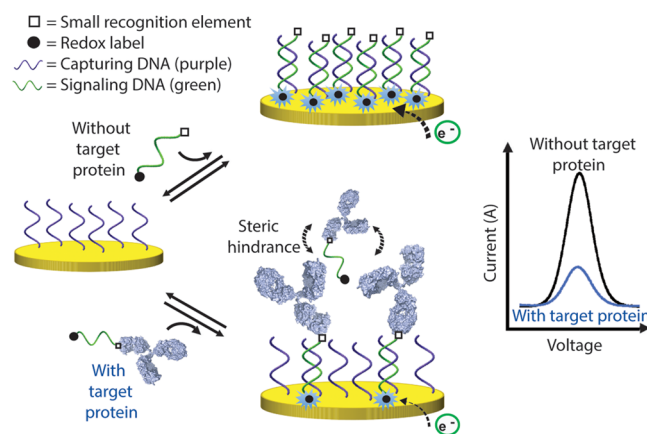


**Figure 1.** Schematic representation of an eSHHA. The eSHHA is composed of a densely packed surface-bound capturing DNA strands (purple) and a free complementary signaling DNA strand (green). The signaling strand is dual labeled with a small recognition element (□) and a signaling redox label [black circle (●): here we used methylene blue to generate the electrochemical readout signal]. In the presence of large target proteins (bottom), the signaling strands are captured by the large macromolecules through binding of the recognition element, which significantly limits their ability to hybridize on the electrode surface due to steric hindrance effect (see Figure S1).

Received: May 12, 2015

Published: September 4, 2015

signaling strands generate a large electrochemical signal by bringing the redox labels (here methylene blue) close to the electrode surface (Figure 1, black peak). In the presence of a large target protein that binds a recognition element on the signaling strand, we hypothesize that fewer copies of this strand will be able to reach the surface-bound capturing strand due to steric hindrance, therefore generating lower electrochemical currents (see proposed model in Figure S1).

As initial proof-of-principle, we first tested our electrochemical steric-hindrance hybridization assay (eSHHA) for the detection of two proteins: antibodies and streptavidin (Figure 2). To do so,

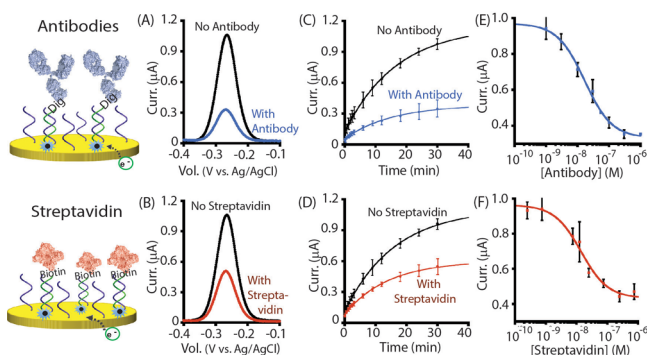


**Figure 2.** Antibody and streptavidin detection using eSHHA. Dig- (top) or biotin- (bottom) labeled signaling strands were used to detect their respective target. (A,B) In presence of target proteins (100 nM), fewer signaling strands reach the gold surface due to steric hindrance, thus generating a lower current. (C,D) The hybridization rate between strands remains similar with or without the protein ( $t_{1/2}$  antibody = 11.6 and 10.5 min; and  $t_{1/2}$  streptavidin = 11.2 and 9.7 min, respectively). (E,F) Dose–response curves of antibody and streptavidin. The errors bars show the standard deviation of current obtained from three electrodes and are dominated by interelectrode variability (see Figure S3).

we designed two 16-base signaling strands labeled at the 3' extremity with methylene blue (redox label) and at the 5' end with the small hapten digoxigenin (Dig) or biotin that are recognized by anti-Dig antibody ( $K_D$  in the low nM)<sup>13</sup> and streptavidin ( $K_D = 40$  fM),<sup>14</sup> respectively (Figure 2). We then immobilized a thiol-modified complementary 16-base DNA capturing strand to a gold surface via the formation of sulfur–gold bond and then backfilled the surface by using 6-mercaptohexanol. In order to improve eSHHA sensitivity and response time, we also optimized the capturing strand density (Figure S2) and the signaling strand concentration (Figure S3). We selected a signaling strand concentration of 100 nM since it generates robust  $\mu$ -amp currents while ensuring detection limits in the low nanomolar (100 nM of target proteins produce maximum response since they sequester 100 nM of signaling strands).

We further tested eSHHA by preparing various samples with increasing concentration of proteins in which 100 nM of signaling strand was added a few seconds before acquisition (<2 s are typically needed for protein attachment on the signaling strand, Figure S4). In absence of target protein, both sensors produced large  $\mu$ A currents in minutes that were reduced by 68% (antibodies) and 52% (streptavidin) in presence of 100 nM of target protein (Figure 2A–D). eSHHA achieved quantitative detection over the typical 100-fold dynamic range<sup>15</sup> for target concentration in the low nM with limits of detection near 10 nM (Figure 2E,F). Dig antibody sensor (Figure 2E) displayed a  $C_{50\%}$  (concentration of target protein when 50% of the sensor signal is

reached) of  $27 \pm 3$  nM, consistent with the fact that half of the signaling strand (50 nM) is expected to be bound by 25 nM of antibodies (two binding sites per antibody). For the streptavidin sensor (Figure 2F), a  $C_{50\%}$  of  $14 \pm 2$  nM was obtained, again consistent with the fact that half of the signaling strand (50 nM) should be bound to 12.5 nM of streptavidin (four binding sites per streptavidin).

Two key controls were designed to support the proposed “steric hindrance” mechanism and to highlight the selectivity of eSHHA. We first verified that no current reduction is observed when the target proteins bind to the hybridized signaling DNA strands (Figure S5). This control also confirms that the lower electrochemical signal obtained in the presence of the target protein is due to fewer signaling strands reaching and hybridizing on the gold surface, rather than to a reduced efficiency in electron transfer resulting from protein binding to the signaling strand (as reported in previous work).<sup>16</sup> Secondly, we confirmed that this signal reduction in the presence of the target protein is produced through the specific binding of the protein to the signaling strand. Indeed, our results show that a signaling strand containing no specific recognition element provides an electrochemical signal of similar intensity whether in presence or absence of target protein (Figure S6). This confirms that the signal reduction observed in eSHHA is not linked to the unspecific protein binding on the electrode's surface.

We then investigated the relationship between the size of the molecule attached to the signaling strand and the electrochemical signal produced by eSHHA. We demonstrated this by comparing the electrochemical signal produced by signaling strands attached to molecules of increasing molecular weights (i.e., from 184 Da and up to 180 kDa) (Figure 3A). For example, the attachment of small size molecules like 2,4-dinitrophenol (184 Da), biotin (244 Da), and digoxigenin (390 Da) to the signaling strand reduced the electrochemical current by 3%, 8%, and 13%, respectively (see also Figure S7). Attachment of a 16-base DNA sequence (5 kDa) reduced the current by 30%, while the binding (through recognition element) of large macromolecules, such as Fab fragment (50 kDa), streptavidin (75 kDa, which includes streptavidin and 4 biotin-bearing signaling strands), and antibodies (such as IgG and IgE  $\sim$  150 kDa) reduced the current by 40%, 50%, and 60%, respectively. We therefore found that the electrochemical signal generated by our eSHHA is inversely correlated with the size of the target macromolecule, following a semilogarithmic relationship (Figure 3A). This result illustrates that eSHHA will provide maximal signal gain reduction when the molecular weight difference between the recognition element and the target macromolecule is maximized. More specifically, when using recognition elements with size varying from 184 Da to 75 kDa to detect IgG antibodies, eSHHA should provide gain reductions ranging from  $-60\%$  to  $-20\%$  in the presence of saturating amount of antibodies, respectively (Figure S8).

Additional evidence supporting the steric hindrance mechanism of eSHHA also came from the demonstration that eSHHA only performs well with a densely packed layer of capturing strands. Accordingly, a poorer performance would be expected with a low covered surface since a target bound or free signaling strand should equally hybridize with a capturing strand. To confirm this, we functionalized several electrodes with varying capturing strand density (Figure 3B,C). We found that the signal gain rapidly (linearly) degrades upon increasing the average distance between the capturing strands (Figure 3C). For example, the electrode with a densely packed layer of capturing strands on its surface (average distance of 5 nm between strands;

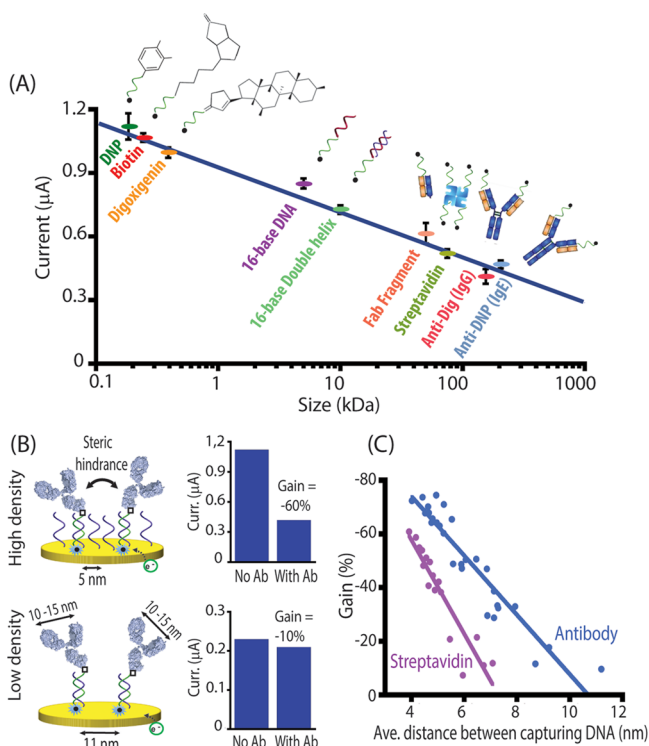


**Figure 3.** (A) eSHHA's electrochemical signal is inversely correlated with the size of the molecule attached on the signaling strand following a semilogarithmic relationship ( $R^2 = 0.96$ ). (B) Optimal eSHHA performance is observed at high capturing strand density when the average distance between capturing strand is smaller than the size of the target protein (5–15 nm). (C) The inverse linear relationship between signal gain and average distance between capturing strands also depends on the target size. For example, larger protein, such as antibodies ( $\sim 12$  nm),<sup>17</sup> produces more steric hindrance and thus can be detected at slightly lower capturing strand density than the smaller streptavidin ( $\sim 5$  nm). Each point represents one electrode (see Figure S3 for typical errors obtained on current and surface density measurements).

lower average distance could not be explored due to drastically slower kinetics, Figure S2) provided a high electrochemical current (1.1  $\mu\text{A}$ ) as well as a  $-60\%$  signal gain reduction in the presence of the target antibody (Figures 3B, top). In contrast, electrodes with a low packed layer of capturing strands (average distance of 11 nm between strands) provided low electrochemical signals (0.2  $\mu\text{A}$ ) and thus a resulting limited signal gain reduction in the presence of antibody ( $-10\%$ ) (Figure 3B, bottom). As expected, the inverse linear relationship between signal gain and average distance between capturing strands was also found dependent on the target size (Figure 3C). This is consistent with the fact that smaller proteins will generate less steric hindrance at the electrode's surface and thus will become undetectable when the average distance between capturing strands is larger than the protein size.

One of the most important advantages of eSHHA is that unlike previously reported single-step methods for detection of proteins, it is selective enough to be employed directly in whole blood. Indeed, eSHHA's performance is nearly identical in terms of gain and kinetic when deployed directly in whole blood or simply in a buffered solution (Figure S9). We also realized a binding curve of anti-digoxigenin antibody directly in whole blood and obtained a  $C_{50\%}$  value (23 nM) that is within the error of the value obtained in pure buffer (27 nM) (Figure S10). Another considerable advantage of eSHHA compared to

previously published electrochemical DNA-based assays for the detection of antibodies<sup>8f,16</sup> is that no rapid signal drift (or change in current) is detected in the first minutes following immersion in whole blood. This is due to the fact that the methylene blue redox label is not present on the electrode's surface but rather on the signaling strand. Therefore, no electrochemical signal will be generated before the signaling strands migrate and hybridize to the capturing strand.

eSHHA can also be adapted for the simultaneous detection of multiple proteins in complex matrices, such as whole blood. We demonstrated this by simultaneously employing, in the same blood sample, several electrodes, each containing different capturing strand sequences. These different sensors, which are each associated with a complementary specific signaling strand linked to a specific recognition element, also display similar kinetics and currents (Figure S11). We demonstrated this multidetection feature by carrying out measurements of two antibodies (anti-Dig and anti-DNP) in whole blood samples (Figure 4). In anti-Dig spiked-blood sample (Figure 4-1), only the electrochemical current of the corresponding blue electrode diminished ( $-60\%$  gain reduction). Similarly, in anti-DNP spiked-blood (Figure 4-2), only the electrochemical current of the corresponding green electrode diminished ( $-50\%$  gain

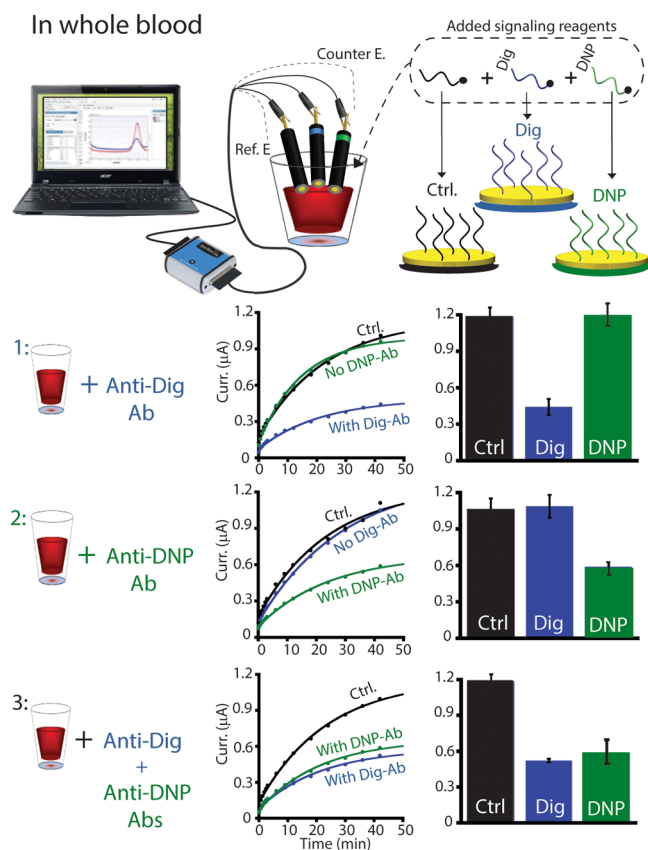


**Figure 4.** eSHHA enables the simultaneous detection of multiple antibodies directly in whole blood. Three electrodes, each functionalized with a specific capturing strand are used to simultaneously detect different antibodies (blue: anti-Dig; green: anti-DNP; black: control electrode). The control electrode (black) hybridizes to a signaling strand bearing no recognition element. The whole blood samples were first spiked with the above-mentioned antibodies (or no antibody), and 100 nM of all the three signaling strand was added a few seconds before acquisition.



reduction). A third blood sample, spiked with both anti-Dig and anti-DNP antibodies (Figure 4-3), generated a eSHHA response in which both the blue and green electrodes gave a significant electrochemical signal gain reduction, while the control “black” electrode remained unchanged. Although the electrochemical signal reached equilibrium only after a 50 min incubation, optimal gain reduction is already attained within the first 10 min (Figure 4B; center). Taken together, these results clearly demonstrate the high potential of the eSHHA as a one-step, easy-to-use assay for the rapid detection of multiple proteins in complex matrices.

We have described a new versatile, highly selective signal transduction mechanism for the one-step detection of proteins based on steric hindrance effect at the nanoscale. This mechanism, which exploits the high specificity and selectivity of DNA hybridization, could in principle be adapted for the detection of any proteins for which we possess a small recognition element.

We show that eSHHA enables the one-step detection of four different macromolecules (with size ranging from 50 to 150 kDa) directly in whole blood. Moreover, eSHHA responds rapidly (<10 min) and sensitively to its targets at low nanomolar concentrations. It displays a signal gain reduction proportional to the macromolecule target size but inversely proportional to the size of the recognition element (e.g., -60% gain reduction when detecting antibodies with recognition elements smaller than 1 kDa, Figure 3A). These results suggest that eSHHA could be adapted to support the use of peptides and other small ligands as recognition elements. eSHHA also enables multiplexed detection of numerous target proteins simultaneously in a sample due to the unique ability of DNA to create numerous specific capturing-signaling pairs (Figure 4).

eSHHA displays significant advantages over comparable existing protein detection technologies. For example, it generates electrochemical signal that are 10 times larger than the recently developed electrochemical DNA-based sensors such as the E-Ab sensors<sup>11a,16</sup> and the bioelectrochemical switches.<sup>8f</sup> Also, since the electrochemical signal is promoted by the specific hybridization of the signaling strand to the electrode, it shows no signal drift when employed directly in whole blood. eSHHA displays also many advantageous features when compared to current methods used for molecular diagnosis such as ELISA, Western blot, and fluorescence polarization assay. It does not require multistep, wash- and reagent-intensive processes, does not need specialized technicians, and requires only a few minutes to perform using an inexpensive portable potentiostat. eSHHA also displays potential advantages over immunochemical dipsticks given its quantitative feature and its ability to support the detection of multiple proteins (at least 8)<sup>11</sup> simultaneously. Given all these advantages, eSHHA emerges as a transduction mechanism of choice for adaptation in POC diagnostic sensors. More generally, this novel, highly selective, steric hindrance based assay could also be adapted into various formats such as a fluorescent sensor, a surface plasmon resonance-based sensor, or even a nanoparticle-based biosensor.

## ■ ASSOCIATED CONTENT

### 📄 Supporting Information

The Supporting Information is available free of charge on the ACS Publications website at DOI: 10.1021/jacs.5b04942.

Experimental materials and methods (PDF)

## ■ AUTHOR INFORMATION

### Corresponding Author

\*a.vallee-belisle@umontreal.ca

### Notes

The authors declare no competing financial interest.

## ■ ACKNOWLEDGMENTS

This work was supported by the Grand Challenges Canada grant CRS3\_0112-01 (A.V.-B.), le Fonds de Recherche Santé du Québec (A.V.-B.), a CRC in Bioengineering and Bionanotechnology, Tier II (A.V.-B.). NSERC (RGPIN-2014-06403 to A.V.-B.), the European Research Council (ERC, 336493 to F.R.), and the EU-IRSES grant “Chimera” (F.R. and A.V.-B.). S.S.M. is a NSERC postdoctoral fellow. We thank PROTEO, the CCVC, and members of the Vallée-Bélisle lab.

## ■ REFERENCES

- (1) (a) Van Weemen, B. K.; Schuur, A. H. W. M. *FEBS Lett.* **1971**, *15*, 232. (b) Engvall, E.; Perlmann, P. *Immunochemistry* **1971**, *8*, 871.
- (2) Towbin, H.; Staehelin, T.; Gordon, J. *Proc. Natl. Acad. Sci. U. S. A.* **1979**, *76*, 4350.
- (3) Jameson, D. M.; Ross, J. A. *Chem. Rev.* **2010**, *110*, 2685.
- (4) (a) Yager, P.; Domingo, G. J.; Gerdes, J. *Annu. Rev. Biomed. Eng.* **2008**, *10*, 107. (b) Yetisen, A. K.; Akram, M. S.; Lowe, C. R. *Lab Chip* **2013**, *13*, 2210.
- (5) Parolo, C.; Merkoci, A. *Chem. Soc. Rev.* **2013**, *42*, 450.
- (6) (a) Banala, S.; Arts, R.; Aper, S. J. A.; Merckx, M. *Org. Biomol. Chem.* **2013**, *11*, 7642. (b) Zhang, H.; Li, F.; Dever, B.; Li, X. F.; Le, X. C. *Chem. Rev.* **2013**, *113*, 2812.
- (7) (a) Gerasimov, J. Y.; Lai, R. Y. *Chem. Commun.* **2010**, *46*, 395. (b) Das, J.; Kelley, S. O. *Anal. Chem.* **2011**, *83*, 1167. (c) Fahie, M.; Chisholm, C.; Chen, M. *ACS Nano* **2015**, *9*, 1089. (d) Golynskiy, M. V.; Koay, M. S.; Vinkenborg, J. L.; Merckx, M. *ChemBioChem* **2011**, *12*, 353. (e) Stratton, M. M.; Loh, S. N. *Protein Sci.* **2011**, *20*, 19. (f) Tian, L.; Heyduk, T. *Anal. Chem.* **2009**, *81*, 5218. (g) Stein, V.; Alexandrov, K. *Trends Biotechnol.* **2015**, *33*, 101.
- (8) (a) Qiu, L. P.; Wu, Z. S.; Shen, G. L.; Yu, R. Q. *Anal. Chem.* **2011**, *83*, 3050. (b) Das, J.; Cederquist, K. B.; Zaragoza, A. A.; Lee, P. E.; Sargent, E. H.; Kelley, S. O. *Nat. Chem.* **2012**, *4*, 642. (c) Lubin, A. A.; Plaxco, K. W. *Acc. Chem. Res.* **2010**, *43*, 496. (d) Lass-Napiorkowska, A.; Heyduk, E.; Tian, L.; Heyduk, T. *Anal. Chem.* **2012**, *84*, 3382. (e) Hu, J.; Yu, Y.; Brooks, J. C.; Godwin, L. A.; Somasundaram, S.; Torabinejad, F.; Kim, J.; Shannon, C.; Easley, C. J. *J. Am. Chem. Soc.* **2014**, *136*, 8467. (f) Vallée-Bélisle, A.; Ricci, F.; Uzawa, T.; Xia, F.; Plaxco, K. W. *J. Am. Chem. Soc.* **2012**, *134*, 15197.
- (9) (a) Vallée-Bélisle, A.; Plaxco, K. W. *Curr. Opin. Struct. Biol.* **2010**, *20*, 518. (b) Gong, L.; Zhao, Z.; Lv, Y. F.; Huan, S. Y.; Fu, T.; Zhang, X. B.; Shen, G. L.; Yu, R. Q. *Chem. Commun.* **2015**, *51*, 979. (c) Zhu, C.; Yang, G.; Li, H.; Du, D.; Lin, Y. *Anal. Chem.* **2015**, *87*, 230.
- (10) (a) Sage, A. T.; Besant, J. D.; Lam, B.; Sargent, E. H.; Kelley, S. O. *Acc. Chem. Res.* **2014**, *47*, 2417.
- (11) White, R. J.; Kallewaard, H. M.; Hsieh, W.; Patterson, A. S.; Kasehagen, J. B.; Cash, K. J.; Uzawa, T.; Soh, H. T.; Plaxco, K. W. *Anal. Chem.* **2012**, *84*, 1098.
- (12) Taft, R. W. In *Steric Effects in Organic Chemistry*; Newman, M. S., Ed.; Wiley: New York, 1956; p 556.
- (13) (a) Tetin, S. Y.; Swift, K. M.; Matayoshi, E. D. *Anal. Biochem.* **2002**, *307*, 84. (b) Chen, G.; Dubrawsky, I.; Mendez, P.; Georgiou, G.; Iverson, B. L. *Protein Eng., Des. Sel.* **1999**, *12*, 349.
- (14) Holmberg, A.; Blomstergren, A.; Nord, O.; Lukacs, M.; Lundeberg, J.; Uhlen, M. *Electrophoresis* **2005**, *26*, 501.
- (15) Vallée-Bélisle, A.; Ricci, F.; Plaxco, K. W. *J. Am. Chem. Soc.* **2012**, *134*, 2876–2879.
- (16) Cash, K. J.; Ricci, F.; Plaxco, K. W. *J. Am. Chem. Soc.* **2009**, *131*, 6955.
- (17) Sosnick, T. R.; Benjamin, D. C.; Novotny, J.; Seeger, P. A.; Trehwella, J. *Biochemistry* **1992**, *31*, 1779.